JACS
JOURNAL OF THE AMERICAN CHEMICAL SOCIETY

ARTICLE

pubs.acs.org/JACS

Probing pH-Dependent Dissociation of HdeA Dimers

Bin W. Zhang,[†] Lucia Brunetti,[‡] and Charles L. Brooks, III[*,†]

[†]Department of Chemistry and Biophysics Program, University of Michigan, Ann Arbor, Michigan 48109, United States

[‡]Department of Molecular Pathologies and Innovative Therapies, Biochemistry Section, Polytechnic University of Marche, 60131 Ancona, Italy

Supporting Information

ABSTRACT: HdeA protein is a small, ATP-independent, acid stress chaperone that undergoes a dimer-to-monomer transition in acidic environments. The HdeA monomer binds a broad range of proteins to prevent their acid-induced aggregation. To understand better HdeA's function and mechanism, we perform constant-pH molecular dynamics simulations (CPHMD) to elucidate the details of the HdeA dimer dissociation process. First the pK_a values of all the acidic titratable groups in HdeA are obtained and reveal a large pK_a shift only for Glu(37). However, the pH-dependent monomer charge exhibits a large shift from −4 at pH > 6 to +6 at pH = 2.5, suggesting that the dramatic change in charge on each monomer may drive dissociation. By combining the CPHMD approach with umbrella sampling, we demonstrate a significant stability decrease of the HdeA dimer when the environmental pH changes from 4.0 to 3.5 and identify the key acidic residue−lysine interactions responsible for the observed pH sensing in HdeA chaperon activity function.

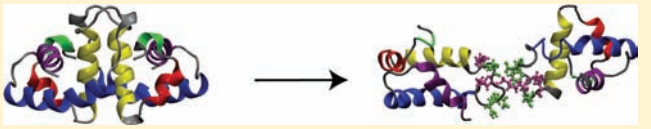

INTRODUCTION

HdeA is a small, ATP-independent, acid stress chaperone that is important for enteric pathogenic bacteria to survive in acidic environments.[1−5] Before reaching the intestine, the bacteria must pass through the mammalian stomach where the pH is usually between 1 and 3. These bacteria have evolved systems to help them tolerate this acidic environment. For example, the glutamate- and arginine-dependent decarboxylases can maintain a near neutral pH inside the inner membrane.[3,4,6−9] However, in the periplasmic space, the pH will decrease to the same value as the environment. In the periplasm, HdeA assists other proteins to combat acid stress.

HdeA prevents acid-induced aggregation of other proteins.[1−5] At neutral pH, HdeA forms a homodimer, as shown in Figure 1. When the pH value of the environment decreases, HdeA undergoes a rapid dimer-to-monomer transition. The HdeA monomer exposes a large hydrophobic surface and becomes chaperone-active. It has been reported that the HdeA monomer is disordered at low pH.[3] Bardwell's group has suggested that its exposed hydrophobic portion and pH-dependent structural plasticity are essential for HdeA to bind a broad range of substrate proteins.[4] The binding with HdeA effectively suppresses the aggregation of denatured substrate proteins. After the bacteria exits the acidic environment, the HdeA monomer releases its substrate protein in a non-native but folding-competent state slowly, so that the concentration of the substrate protein will remain below the aggregation threshold. In this environment, the binding partner folds back to its native structure.[5] In contrast with the emergence of these exciting experimental reports about HdeA's function and mechanism, few detailed atomic studies exist and no simulations have been performed for this small protein, although HdeA has been used as a test protein for protein structure prediction at neutral pH.[10] One possible reason is that simulations at specific pH values are still a challenging problem.

It is important to develop simulation techniques that treat solution acidity as a controllable factor. Like temperature and pressure, pH is a key thermodynamic variable, and it can strongly affect the structure and function of proteins and other biomolecules. The influences of acidity and the titration behavior of a protein are key experimental handles on the structure and function of biological molecules.[11,12]

Significant recent progress has been made in the development of constant pH simulation techniques, making simulations of pH dependent phenomena possible. Descriptions and details of these developments can be found in current review papers.[12,13] For completeness we provide a brief overview of these approaches in what follows. To obtain the pK_a of the titratable sites in a biological molecule, thermodynamic integration (TI) and other methods are used to calculate the free energy difference between the protonated and unprotonated states.[14] With the energy or distribution differences between the protonated and unprotonated states, MC and mixed MC/MD constant pH simulations have been developed using discrete protonation states.[15−20] Lee et al. described a constant pH molecular dynamics (CPHMD) technique using continuous protonation states based on λ dynamics.[21] In their model, the two ends λ = 0 and λ = 1 represent the completely protonated and unprotonated states. Later, Khandogin and Brooks added another dimension x, representing the proton tautomers.[22] CPHMD was combined with the replica-exchange method (REX-CPHMD)[23,24] and achieved even better convergence of

Received: June 28, 2011
Published: October 25, 2011

the protonation states.[25] The REX-CPHMD simulation package has been included in CHARMM[26] and the MMTSB toolset,[27] and applied to study pH-dependent peptide folding[28] and the aggregation of Alzheimer's β-amyloid peptides.[29]

In this first simulation paper studying the protein HdeA, our work is focused on determining the pK_a values of all titratable residues in the HdeA dimer and monomer and on obtaining the potential of mean force for the dimer-to-monomer transition. Later a characterization of the physical forces that lead to pH-dependent conformational changes will be discussed. We note that these are the first calculations that attempt to explain the pH-dependent dimer−monomer equilibrium.

MATERIALS AND METHODS

HdeA. The PDB file for the protein HdeA (1BG8)[1] was downloaded from the protein data bank.[30] The HdeA dimer (chains A and B) in the PDB file was used for our simulation. Because of the high disorder of the N- and C-terminal residues, each monomer contains 76 residues (10−85) out of 89.[1]

pK_a Calculations. The pK_a of all the titratable groups can be obtained by CPHMD simulations (see Supporting Information).[21,22] To enhance the simulation for the fully protonated (λ = 1) and unprotonated (λ = 0) states in the simulation, a cutoff value is used. The definition used in our analysis is

$$\begin{aligned} N^{\mathrm{U}} &= N(\lambda > 0.9; x < 0.1 \text{ or } x > 0.9) \\ N^{\mathrm{P}} &= N(\lambda < 0.1; x < 0.1 \text{ or } x > 0.9) \end{aligned} \quad (1)$$

where N is the number of times a state is occupied in a simulation. The fractional population of unprotonated states S^{U} is given by

$$S^{\mathrm{U}} \approx \frac{N^{\mathrm{U}}}{N^{\mathrm{U}} + N^{\mathrm{P}}} \quad (2)$$

After getting S^{U} of a titrating group at different pH values, the pK_a value is obtained from fitting the Henderson-Hasselbach equation

$$S^{\mathrm{U}} = \frac{1}{1 + 10^{n(\mathrm{p}K_a - \mathrm{pH})}} \quad (3)$$

where n is the Hill coefficient. To find the pK_a of all the titratable groups in HdeA, the fractional population of unprotonated states S^{U} was obtained for 10 different pH conditions (pH = 2.0,2.5,3.0,3.5,4.0,5.0,6.0,7.0, 8.0,9.0). The REX-CPHMD simulation for each pH used 24 replicas for the dimer with an exponential temperature spacing between 298 and 450 K, and used 16 replicas for the monomer with an exponential temperature spacing between 298 and 420 K. A conformational exchange was attempted between adjacent replicas every 2*ps*. The salt concentration was fixed at 0.15*M* in all simulations to represent typical salt concentrations in experimental studies.

Umbrella Sampling. The dimer-to-monomer transition of HdeA was studied using the CPHMD simulations[21,22] and the umbrella sampling method[31−33] to obtain the potential of mean force (PMF) as a function of the distance between the centers of mass of the two monomers (D_{com}). A harmonic biasing potential

$$U(D_{\mathrm{com}}) = \frac{1}{2} k(D_{\mathrm{com}} - D_{\mathrm{min}})^2 \quad (4)$$

was applied in the CPHMD simulations, where k is the force constant, which was set to 10 kcal/(mol · Å^2), and D_{min} is the minimal potential position. D_{min} can be written as:

$$D_{\mathrm{min}} = D_0 + \Delta D \quad (5)$$

where D_0 is the initial D_{com} found from the PDB file (18.1 Å). To obtain the PMF at a specified pH value, multiple Langevin CPHMD simulations were run at 300 K using $\Delta D = n \times 0.8$ Å, where n is an integer ranging from −3 to 40. Although the truncation distance for nonbonded interactions in the simulations was 20.0 Å, the HdeA monomers still interact at distances of ΔD = 20.0 Å because of rotations and conformational fluctuations of loop regions. Consequently, we compute the PMF curves out to a maximum value of ΔD = 32.0 Å (D_{min} = 50.1 Å), where they appear to have plateaued.

For the Langevin dynamics, a friction coefficient of 5 ps^{-1} was used. The salt concentration was 0.15 M. The SHAKE algorithm was applied so that the stepsize for dynamics was increased to 2 fs. Every simulation was run for 3 ns, the first 1 ns was treated as the relaxation time and was not used for the PMF calculation. WHAM[34−36] was used to combine the PMF across the whole region.

Table 1. Calculated pK_a Values for HdeA Residues at T = 298 K

residue	pK_a dimer chain A	pK_a dimer chain B	pK_a monomer
Glu(19)	3.6	3.8	3.8
Asp(20)	2.6	2.6	3.8
Asp(25)	3.1	3.1	2.7
Glu(26)	4.4	4.3	4.0
Glu(37)	**6.9**	**6.5**	5.3
Asp(43)	3.1	2.6	3.7
Glu(46)	3.4	3.5	3.7
Asp(47)	3.6	4.1	4.2
Asp(51)	2.7	2.9	3.8
Asp(69)	3.6	3.4	3.8
Asp(76)	2.8	2.7	3.5
Glu(81)	4.2	4.0	4.0
Asp(83)	3.1	3.1	3.7

RESULTS AND DISCUSSION

Results. The pK_a values of acidic residues (Asp and Glu) in the HdeA dimer and monomer were obtained from analysis of REX-CPHMD simulations and are summarized in Table 1. There are a total of 8 aspartic acid residues and 5 glutamic acid residues in the HdeA monomer. The pK_a of an isolated aspartic acid side chain is 3.9 and the pK_a of an isolated glutamic acid side chain is 4.3. Compared with these values, we found that most titratable residues have small negative pK_a shifts (ΔpK_a < 2.0), except for Glu(37). The pK_a of the Glu(37) side chain in the HdeA dimer increases to 6.7. There are minor differences between the pK_a values of the same residue in chain A and B, which arises from the asymmetry of the HdeA dimer during the molecular dynamics simulations and from the precision of pK_a values arising from the CPHMD simulations. There are also nine lysine residues in the HdeA monomer. An isolated lysine side chain has a pK_a of 10.5. We assumed the lysine residues are in the protonated state when the pH is lower than 8. The pK_a values of the lysine residues in the HdeA dimer and monomer were not studied in this paper. There are no histidine or arginine residues in HdeA.

The umbrella sampling method was used to obtain the potential of mean force (PMF) as a function of the change of the distance between the centers of mass of the two monomers, ΔD_{com}. The results for pH values 2−7 are shown in Figure 2. All of the PMF curves have been shifted such that the lowest free energy, which occurs in the dimer state, is at 0 kcal/mol. From the results displayed in Figure 2, the binding free energy curves

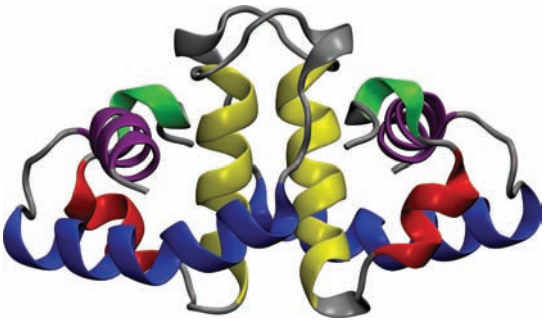

Figure 1. HdeA dimer. Each HdeA monomer consists primarily of 4 helices. The dimer interface is comprised of the helix B (yellow), the loop between helix B (yellow) and helix C (blue) and part of the N terminal tail of each monomer.[1]

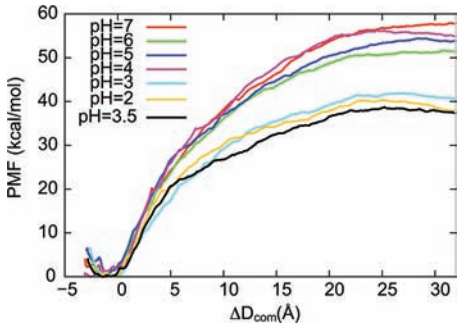

Figure 2. Potential of mean force (PMF) as a function of the distance between the centers of mass of the two monomers at pH values between 2 and 7. The change in the distance between the two monomers, ΔD_{com}, is defined as $\Delta D_{com} = D_{com} - D_0$ where D_{com} represents the distance between the centers of mass of the monomers and D_0 is the reference value of D_{com} taken from the PDB file (18.1 Å).

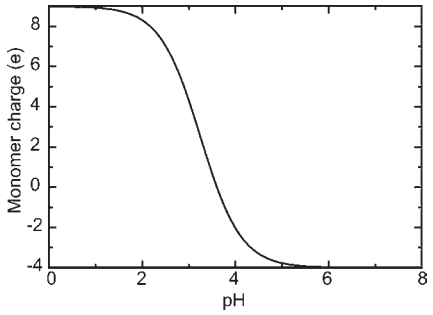

Figure 3. Overall charge on the HdeA monomer as a function of pH.

(PMFs) can be divided into a stable group (pH ≥ 4) and a less stable group (pH ≤ 3.5; see also Figure S1, Supporting Information).

On the basis of the pK_a values presented above, we calculated the net charge of the HdeA monomer at different pH values. This is shown in Figure 3. As mentioned above, in the region 0 < pH < 8, all the lysine residues are assumed to be protonated and carry a unit positive charge. The aspartic acid and glutamic acid residues are in the unprotonated state when the pH equals 8 and have a negative charge. So the total charge at pH = 8 is $-4e$. When the pH drops to 0, all the aspartic acid and glutamic acid residues become protonated so the total charge of the HdeA monomer is $+9e$. The net charge of the HdeA monomer is $-4e$ at pH = 7, and $+4e$ at pH = 3. Considering a simplified Born model, two spheres with charges of $+4e$ will have the same PMF as two spheres with charges $-4e$. For HdeA, although the absolute charges remain the same, the PMF curves are different at pH = 3 and pH = 7 (see Figure 2). This indicates that the pH sensing mechanism in HdeA is not simply related to the overall charge on a monomer.

DISCUSSION

The calculations of the free energy curves describing HdeA dissociaiton (the PMFs) are shown in (Figure 2). They clearly show that the HdeA dimer becomes destabilized when the pH decreases. When the monomers are separated by 32.0 Å, the PMF reaches a plateau near 40 kcal/mol at low pH . The PMF is expected to decrease after the monomers are completely dissociated because of the gain in translational and rotational entropy.[37] According to previous reports, this entropy gain is anticipated to be on the order of 50−100 cal/(mol · K).[38−40] Thus at 300 K the PMF is expected to decrease 15−30 kcal/mol upon dissociation. Second, the structure of the HdeA monomer becomes disordered, as has been observed in experiments at low pH,[3,4] which would further lower the PMF due to protein configurational entropy in the unfolded state. This suggests that the stability of the monomer state is likely to be favored, or at least competitive with the dimer state when the environmental pH is low.

What then causes the dimer-to-monomer transition of HdeA? A reasonable explanation is that the change of the interactions between charges causes the dissociation. As discussed previously, when the pH equals 7, in the HdeA monomer there are 9 positive and 13 negative charges. At this time the attractions between the positive and negative charges in different monomers and the large hydrophobic area in the interface make the dimer stable. When the pH is decreased below 3.5, most of the negative charges are neutralized so it becomes easier for the monomers to separate. Thus, the lysine residues that favorably interact with the negatively charged acidic residues across the dimer interface at near neutral pH values are now less attracted to the neutral form of these residues. This suggests that the pH sensing mechanism may involve the pairs of positively and negatively charged side chains that can interact across the dimer interface.

The HdeA dimer becomes less stable between pH = 4 and 3.5 as indicated by the larger shifts in the PMF curves at longer distances. The change in the PMF is relatively smaller for pH values outside this region. The difference in the PMF between pH = 3 and 7 suggests that the intermonomer interactions are determined by the distribution of charges in HdeA rather than the absolute net change. Apparently in HdeA, some titratable groups play more important roles in dimer dissociation than others. From our umbrella sampling trajectories with ΔD_{com} = 0 Å and pH = 7, we calculated the arithmetic mean of distances between each acidic residue in one monomer and all the lysine residues in the other monomer (see Tables S1 and S2, Supporting Information). Among all the acidic residues, we found that those in the loop connecting helix B and C, Asp(43), Glu(46), Asp(47) and Asp(51) in one monomer, are in close proximity to positive lysine clusters in the other monomer. There are three lysine clusters in the HdeA monomer. They are located in (i) the N terminus, (ii) the loop connecting helix B and C, and (iii) helix D and the loop connecting helix C and D. Figure 4 shows the positions of Asp(43), Glu(46), Asp(47)

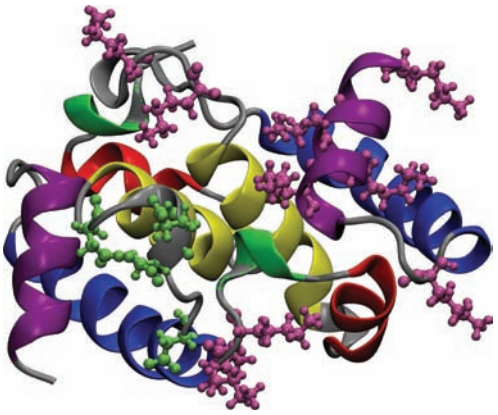

Figure 4. Positions of Asp(43), Glu(46), Asp(47) and Asp(51) residues (green – ball and stick) in one monomer and all the lysine residues (purple – ball and stick) in the other monomer from PDB file 1BG8. Asp(43), Glu(46), Asp(47) and Asp(51) are in proximity to all the positive lysine clusters in the other monomer.

and Asp(51) in one monomer and all the lysine residues in the other monomer. Considering that the electrostatic force depends on the inverse-square of distance between charges, these residues are likely the key elements for the stability and pH sensing of the HdeA dimer. The pK_a values of these acidic residues also suggest that they are responsible for the PMF difference between pH = 4 and 3.5. According to Eq. 3 the Henderson-Hasselbach equation, the fractional population of the unprotonated state changes most around the pK_a value. As observed from the data in Table 1, the pK_a values of Glu(46) and Asp(47) in the dimer are in the region $3.5 \leq \text{pH} \leq 4.0$. As the HdeA monomers separate during dissociation, the pK_a values of these residues will shift to those calculated for the HdeA monomer, where all four acidic residues in the loop connecting helix B and C have pK_a values in or adjacent to the region $3.5 \leq \text{pH} \leq 4.0$. Finally, from an analysis of the conformations of the proteins during our umbrella sampling, we find that the loops connecting helices B and C in one monomer move toward the other monomer as the distance between the centers of mass of the two monomers is increased (see Supporting Information for data and an illustration).

The analysis of the pK_a of the acidic residues and the structure suggest the interaction between the negative charges in the loop connecting helix B and C of one monomer and the positive charges from the lysine clusters of the other monomer is essential for the stability and pH sensing of the HdeA dimer. The neutralization of these negative charges seems to trigger dimer dissociation. We analyzed 48 sequences of HdeA and HdeB homologues (see Supporting Information for data). Most of these homologues have multiple glutamic acid or aspartic acid residues among the positions of the loop connecting helix B and C, showing 6% similarity (aspartic acid or glutamic acid residue) for the position of Asp(43), 36% similarity for Glu(46), 70% similarity for Asp(47) and 49% similarity for Asp(51). The distribution of positively charged residues is also conserved. All the homologues are highly positively charged at the N and C termini. Most of them have 1–3 positively charged residues in the loop connecting helix B and C, and there is 74% sequence similarity (lysine or arginine residues) at the position of Lys(44). It seems that the mechanism to trigger the dimer dissociation of HdeA may be common for this type of protein.

It is highly possible that the neutralization of negative charges is also the mechanism causing the monomer to be disordered and flexible.[3] The attraction between the positive and negative charges may not only make the dimer stable but also make the monomer compact and folded. It was reported that the HdeA monomer at low pH retains its secondary structure but loses its tertiary structure.[4] Our PMF calculations indicate that it is easier to separate the HdeA dimer when the pH is lower than 4. To explore further the stability of the monomer at low pH, 8 ns CPHMD simulations of the HdeA monomer were carried out at pH = 1, 2, 3 and 4. From these simulations (data not shown), we found that the monomer remained largely folded; however, the rmsd increased at lower pH values, suggesting that the HdeA monomer becomes more flexible in the increasingly acidic environment. In the simulations, we found that two of the acidic residues, Glu(19) and Asp(20) in helix A of HdeA, are adjacent to the lysine cluster in helix D and the loop connecting helix C and D. We also found that these helix A residues are highly conserved, with 62 and 81% similarity, respectively, in all of the HdeA and HdeB homologues. As we previously noted, the C terminus of all of the homologues is highly positively charged. It is reasonable to suggest that in HdeA and HdeB the interaction between these two groups comprise interactions that hold helix A and D together. When Glu(19) and Asp(20) become protonated at pH < 3, these two helices will have greater flexibility and the monomer will expose more of its hydrophobic surface. In this state, the chaperone function can be fully activated.[5] To understand better the ensemble of conformations that represent the HdeA monomer in low pH environments, more specialized and advanced simulations (outside the scope of the present study) are required.

The interactions between all titratable residues in a biomolecule cause their pK_a changes.[41] Sometimes the major contribution is obvious. For example, in the HdeA dimer the distance between Asp(20) and Lys(11) (in the N terminus) is around 5 Å. The negative shift of Asp(20) probably comes from the nearby positive charge of Lys(11). The most interesting pK_a result is the large positive shift of Glu(37) (from 4.3 to 6.7), although it does not seem to be critical for the dissociation of the HdeA dimer. Table 1 includes the pK_a values in the HdeA monomer, which are calculations in a hypothetical environment since the HdeA monomer only exists at low pH. The N terminus, which used to be one part of the interface of dimer, has more freedom in the CPHMD simulation of HdeA monomer. This explains why the pK_a of Asp(20) shifts back to 3.8. But the major part of the monomer remains intact. Therefore, the pK_a values measured in the HdeA monomer are anticipated to be indicative of what will happen if all the charges in the other side of the HdeA dimer are totally neutralized. The charge distribution in Glu(37)'s own monomer already shifts its pK_a from 4.3 to 5.3. Considering Glu(37)'s location, it is not surprising that its pK_a shifts further in the HdeA dimer. Glu(37) is located in the middle of helix B, which is also one part of the dimer interface, see Figure 1. The two Glu(37)s are adjacent to each other because of the symmetry of the dimer. The overlapped influence from both monomers cause Glu(37)'s large pK_a shift. The unusual pK_a of Glu(37) probably also serves HdeA monomeric function. Glu(37) carries negative charge close to the hydrophobic dimer interface, its early protonation guarantees that the HdeA monomer can bind other proteins more efficiently. If its deprotonation works as a trigger to release bound protein, its positively shifted pK_a ensures that this separation will happen when the pH is higher than 5.3, so the

chaperoned protein has a better chance to fold back into its native state.

The CPHMD method is a powerful technique to study biological molecules in specific pH environments. Compared with the traditional fixed protonation state strategies, the CPHMD approach has the ability to simulate protonation state equilibrium and the interactions between all titratable groups with modest computational cost.[13] More importantly, the CPHMD approach is not only a pK_a calculator, it also captures the coupling between the protonation of titratable groups and the conformational changes of the biological molecule.[13] The CPHMD method successfully highlighted the difference of the PMF corresponding to the dissociation of the HdeA dimer at different pH values. By adding continuous variables to describe the states of titratable sites, the CPHMD approach is a regular MD simulation in a higher dimensional space following its hybrid potential function. In the simulation there is no discontinuous energy or force. Therefore other techniques, which can be combined with regular MD simulations, can be applied with the CPHMD method without difficulty, for example, the umbrella sampling approach used in this paper.

Other interesting topics remain open, which can be studied by CPHMD simulations in the future. Our work shows how essential the acidic groups are for HdeA's acid stress function. Depending on their locations and pK_as, those titratable groups work in different phases. The present data suggest that the acidic residues in the loop connecting helix B and C, Asp(43), Glu(46), Asp(47) and Asp(51) are the pH sensors responsible for the dissociation of the HdeA dimer. Our data also provide several interesting suggestions which need further investigation. For example, after dissociation, the HdeA monomer will remain in a disordered state with the ability to bind a broad range of proteins.[3,4] The protonation of Glu(19) and Asp(20) seems to contribute to the flexibility of monomeric HdeA in a low pH environment. Glu(37), which has the significant positive pK_a shift, is probably involved in the functional aspects of monomer binding and releasing of other proteins. CPHMD simulation could be utilized to understand more of the details of these phenomena and the roles played by all these acidic titratable groups.

CONCLUSIONS

We applied the CPHMD approach to study the HdeA protein, a small, ATP-independent, acid stress chaperone. The HdeA homodimer dissociates when the environment becomes acidic. The HdeA monomer has a disordered structure and can bind to a broad range of proteins to prevent the acid-induced aggregation of these proteins. We obtained the pK_a values of all thirteen acidic groups in the HdeA dimer and monomer, and found that except for Glu(37), all titratable residues have only minor pK_a decreases relative to their intrinsic pK_a values. The pK_a of the Glu(37) side chain in the HdeA dimer increases from 4.3 to 6.7. To study the dimer-to-monomer transition, umbrella sampling was used to obtain the potential of mean force as a function of the distance between the centers of mass of the two monomers. Our results show that the HdeA dimer stability decreases significantly when the pH of the environment drops from 4 to 3.5. We found four titratable groups, Asp(43), Glu(46), Asp(47) and Asp(51), have their pK_a in or adjacent to this region and are in proximity to all three positively charged clusters in the other monomer. They are likely the key elements that trigger the dissociation of the HdeA dimer.

ASSOCIATED CONTENT

Supporting Information. Constant-pH molecular dynamics simulation theory, test of convergence, distance between acidic titratable residue and lysine residue, snapshot in the umbrella sampling, sequence analysis and Complete ref 26. This material is available free of charge via the Internet at http://pubs.acs.org.

AUTHOR INFORMATION

Corresponding Author
brookscl@umich.edu

ACKNOWLEDGMENT

The NIH via GM057513 is acknowledged. We acknowledge extensive discussions with Professor James Bardwell and Dr. Timothy Tapley. Additionally B.W.Z. thanks the Brooks' group members and especially Dr. Jennifer Knight for assistance with the manuscript.

REFERENCES

(1) Yang, F.; Gustafson, K. R.; Boyd, M. R.; Wlodawer, A. *Nat. Struct. Mol. Biol.* **1998**, *5*, 763–764.
(2) Gajiwala, K. S.; Burley, S. K. *J. Mol. Biol.* **2000**, *295*, 605–612.
(3) Hong, W.; Jiao, W.; Hu, J.; Zhang, J.; Liu, C.; Fu, X.; Shen, D.; Xia, B.; Chang, Z. *J. Biol. Chem.* **2005**, *280*, 27029–27034.
(4) Tapley, T. L.; Körner, J. L.; Barge, M. T.; Hupfeld, J.; Schauerte, J. A.; Gafni, A.; Jakob, U.; Bardwell, J. C. A. *Proc. Natl. Acad. Sci. U.S.A.* **2009**, *106*, 5557–5562.
(5) Tapley, T. L.; Franzmann, T. M.; Chakraborty, S.; Jakob, U.; Bardwell, J. C. A. *Proc. Natl. Acad. Sci. U.S.A.* **2010**, *107*, 1071–1076.
(6) Biase, D. D.; Tramonti, A.; Bossa, F.; Visca, P. *Mol. Microbiol.* **1999**, *32*, 1198–1211.
(7) Castanie-Cornet, M.-P.; Penfound, T. A.; Smith, D.; Elliott, J. F.; Foster, J. W. *J. Bacteriol.* **1999**, *181*, 3525–3535.
(8) Audia, J. P.; Webb, C. C.; Foster, J. W. *Int. J. Med. Microbiol.* **2001**, *291*, 97–106.
(9) Foster, J. W. *Nat. Rev. Microbiol.* **2004**, *2*, 898–907.
(10) Papoian, G. A.; Ulander, J.; Eastwood, M. P.; Luthey-Schulten, Z.; Wolynes, P. G. *Proc. Natl. Acad. Sci. U.S.A.* **2004**, *101*, 3352–3357.
(11) Alberty, R. A. *Thermodynamics of Biochemical Reactions*; Wiley-Interscience: New York, 2003.
(12) Mongan, J.; Case, D. A. *Curr. Opin. Struct. Biol.* **2005**, *15*, 157–163.
(13) Chen, J.; Brooks, C. L., III; Khandogin, J. *Curr. Opin. Struct. Biol.* **2008**, *18*, 140–148.
(14) Simonson, T.; Carlsson, J.; Case, D. A. *J. Am. Chem. Soc.* **2004**, *126*, 4167–4180.
(15) Bürgi, R.; Kollman, P. A.; van Gunsteren, W. F. *Proteins: Struct., Funct., Genet.* **2002**, *47*, 469–480.
(16) Baptista, A. M.; Teixeira, V. H.; Soares, C. M. *J. Chem. Phys.* **2002**, *117*, 4184–4200.
(17) Dlugosz, M.; Antosiewicz, J. M.; Robertson, A. D. *Phys. Rev. E* **2004**, *69*, 021915.
(18) Dlugosz, M.; Antosiewicz, J. M. *Chem. Phys.* **2004**, *302*, 161–170.
(19) Mongan, J.; Case, D. A.; McCammon, J. A. *J. Comput. Chem.* **2004**, *25*, 2038–2048.
(20) Williams, S. L.; de Oliveira, C. A. F.; McCammon, J. A. *J. Chem. Theory Comput.* **2010**, *6*, 560–568.
(21) Lee, M. S.; Freddie, R. S.; Brooks, C. L., III *Proteins: Struct., Funct., Bioinf.* **2004**, *56*, 738–752.
(22) Khandogin, J.; Brooks, C. L., III *Biophys. J.* **2005**, *89*, 141–157.
(23) Swendsen, R. H.; Wang, J.-S. *Phys. Rev. Lett.* **1986**, *57*, 2607–2609.

(24) Zuckerman, D. M.; Lyman, E. *J. Chem. Theory Comput.* **2006**, *2*, 1200–1202.
(25) Khandogin, J.; Brooks, C. L., III *Biochemistry* **2006**, *45*, 9363–9373.
(26) Brooks, B. R.; et al. *J. Comput. Chem.* **2009**, *30*, 1545–1614.
(27) Feig, M.; Karanicolas, J.; Brooks, C. L., III *J. Mol. Graph. Model.* **2004**, *22*, 377–395.
(28) Khandogin, J.; Chen, J.; Brooks, C. L., III *Proc. Natl. Acad. Sci. U.S.A.* **2006**, *103*, 18546–18550.
(29) Khandogin, J.; Brooks, C. L., III *Proc. Natl. Acad. Sci. U.S.A.* **2007**, *104*, 16880–16885.
(30) Berman, H. M.; Westbrook, J.; Feng, Z.; Gilliland, G.; Bhat, T. N.; Weissig, H.; Shindyalov, I. N.; Bourne, P. E. *Nucleic Acids Res.* **2000**, *28*, 235–242.
(31) Frenkel, D.; Smit, B. *Understanding Molecular Simulation: From Algorithms to Applications*, 2nd ed.; Academic Press: New York, 2001.
(32) Torrie, G. M.; Valleau, J. P. *J. Comput. Phys.* **1977**, *23*, 187–199.
(33) Northrup, S. H.; Pear, M. R.; Lee, C. Y.; McCammon, J. A.; Karplus, M. *Proc. Natl. Acad. Sci. U.S.A.* **1982**, *79*, 4035–4039.
(34) Kumar, S.; Rosenberg, J. M.; Bouzida, D.; Swendsen, R. H.; Kollman, P. A. *J. Comput. Chem.* **1992**, *13*, 1011–1021.
(35) Boczko, E. M.; Brooks, C. L., III *J. Phys. Chem.* **1993**, *97*, 4509–4513.
(36) Kumar, S.; Rosenberg, J. M.; Bouzida, D.; Swendsen, R. H.; Kollman, P. A. *J. Comput. Chem.* **1995**, *16*, 1339–1350.
(37) Woo, H.-J.; Roux, B. *Proc. Natl. Acad. Sci. U.S.A.* **2005**, *102*, 6825–6830.
(38) Finkelstein, A. V.; Janin, J. *Protein Eng.* **1989**, *3*, 1–3.
(39) Tidor, B.; Karplus, M. *Proteins: Struct., Funct., Genet.* **1993**, *15*, 71–79.
(40) Tamura, A.; Privalov, P. L. *J. Mol. Biol.* **1997**, *273*, 1048–1060.
(41) Onufriev, A.; Case, D. A.; Ullmann, G. M. *Biochemistry* **2001**, *40*, 3413–3419.